Journal of Applied Electrochemistry (2005) 35:1–7
DOI 10.1007/s10800-004-0175-9

Selection of an oxidant for copper chemical mechanical polishing: Copper-iodate system

M. ANIK
Metallurgy Institute, Osmangazi University, 26480 Eskisehir, Turkey (e-mail: manik@ogu.edu.tr)

Received 19 September 2003; accepted in revised form 27 May 2004

Key words: CMP, copper, iodate, mixed potential theory

Abstract

Diagnostic criteria were developed to elucidate the reduction mechanism of an oxidant on a copper (Cu) surface at the corrosion potential. The corrosion potential of Cu was measured for various pH and iodate (IO_3^-) concentrations using the rotating disk electrode technique. According to the measured corrosion potentials, IO_3^- was an effective CMP oxidant only below pH 3. Application of the diagnostic criteria on the Cu – IO_3^- system showed that the reduction of IO_3^- on Cu was under the mixed kinetic and diffusion control at the corrosion potential below pH 3. Above pH 3, however, the anodic process dominated over the cathodic process.

1. Introduction

Copper (Cu) has been chosen as a substitute for aluminum in multi-level interconnections due to its low resistivity and high electromigration resistance [1]. The dual damascene technique coupled with chemical mechanical polishing (CMP) is used for the patterning of Cu layers [2]. Therefore CMP of Cu interconnects plays a critical role in the manufacture of integrated circuits. Typical CMP slurries contain oxidants, etchants and abrasive particles. During CMP of Cu, an oxidant passivates the Cu surface and the passivation layer formed in protruding regions is removed by the mechanical action of abrasive particles [3]. The exposed metal surface in these protruding regions is also removed by the chemical action of an etchant.

Effective planarization of the wafer surface can only be accomplished if fundamentals of the CMP process are understood. There are several CMP models [4–8]. These models, however, have been mainly concerned with the mechanical aspects of the process. The chemical effects, especially for metal CMP, also play an important role [2, 3, 9–15]. During the metal CMP process, the metal oxidation is driven by the reduction of an oxidant (cathodic reaction) on the metal surface; at steady-state, anodic current = cathodic current. Therefore, the extension of mixed potential theory [16–19] to the chemical aspects of CMP may help in future modeling of this process.

The iodate (IO_3^-) ion is one of the important oxidants present in commercial CMP slurries [11–13, 20, 21]. The reduction behavior of IO_3^- on tungsten [22, 23] and on copper (M. Anik, submitted) have been reported previously. In this study, in order to observe the reduction characteristics of IO_3^- on Cu at the corrosion potential diagnostic criteria are developed based on mixed potential theory [17, 18] and potential measurements are carried out using a rotating disk electrode.

2. Materials and methods

2.1. *Materials*

A copper (Cu) rod 0.635 cm in diameter (99.998% purity) was obtained from Aldrich. Reagent grade KIO_3, K_2SO_4, H_3PO_4, KOH and H_2SO_4 were purchased from Aldrich. All the aqueous solutions were prepared from doubly distilled water. The water was deoxygenated by bubbling argon before experiments and purging was continued throughout the experiments. All test solutions contained 0.1 M H_3PO_4 as a pH buffer and 0.1 M K_2SO_4 as supporting electrolyte. The pH of the test solutions was adjusted with KOH or H_2SO_4.

2.2. *Methods*

The Cu electrode used in the electrochemical experiments was embedded in a cylindrical piece of Teflon. To block the crevice between the Teflon holder and the electrode epoxy was applied and subsequently allowed to harden in vacuum. The exposed electrode surface (0.317 cm^2) was ground with 1200 grit grinding paper and polished with 1 μm diamond paste just prior to each experiment. The polished electrode was rinsed with

acetone and double distilled water to eliminate traces of diamond paste from the surface.

A standard three-electrode system consisting of the copper working electrode, a platinum wire mesh counter electrode, and a saturated calomel reference electrode was used. The counter electrode was separated from the main compartment by enclosing it in a fritted glass tube. A Gamry model PC4/300 mA potentiostat/galvanostat controlled by a computer by a model DC105 DC Corrosion Analysis software was used. Rotating disc electrode (RDE) experiments were carried out using an EG & G model 616 rotating assembly. The electrical connection was provided from the back of the electrode by attaching it to the RDE assembly. All experiments were performed in a 200 ml glass cell.

In corrosion potential measurements the electrode was kept in the test solution for about 1 h in order to achieve steady-state and then the experiment was run. The rotation speed was varied between 0 and 2500 rpm, with increments of 500 rpm. Unless indicated otherwise, all potentials are referred to the saturated calomel reference electrode, SCE (SCE, +0.241 V vs SHE). All experiments were conducted at laboratory temperature (25 ± 0.5 C).

3. Results and discussion

3.1. *Electrochemical equilibria in I–H_2O and Cu–H_2O systems*

The relative stability regions of the aqueous substances in I–H_2O and Cu–H_2O systems are shown in the potential (Eh)–pH diagrams, presented in Figures 1 and 2, respectively. The data used to prepare these diagrams are tabulated in Table 1 [24, 25]. As shown in Figure 1, at very high potentials protonated and deprotonated forms of IO_4^- and IO_5^{3-} are the main I (VII) species in the acidic and basic regimes, respectively. A relatively small HIO_4 (aq) region appears below pH 1.6. At lower potentials, I (V) exists as HIO_3 below pH 1 and as IO_3^- above this pH. The reduction products of IO_3^-, i.e., I_2 and I^-, appear (just below the upper water stability line) in Figure 1. Figure 2 shows that the cupric ion (Cu^{2+}) is the only species in the acidic regime at all oxidizing conditions. In neutral to basic solution, CuO replaces Cu^{2+} as the stable Cu(II) species while a narrow region of cuprous oxide (Cu_2O; Cu(I)) is sandwiched between Cu and CuO at intermediate oxidizing conditions. Elemental Cu is stable under all reducing conditions in Figure 2.

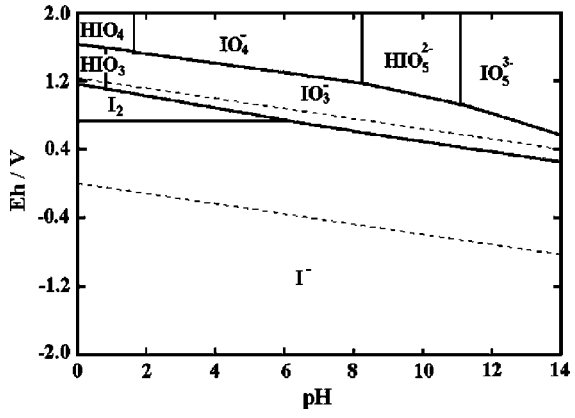

Fig. 1. Eh–pH diagram for I – H_2O system; [I] = 10^{-3} M.

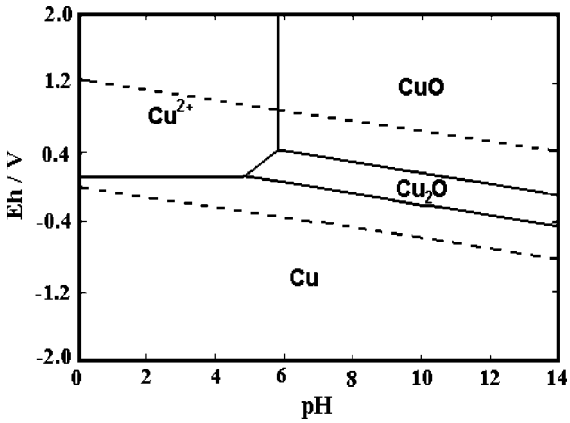

Fig. 2. Eh–pH diagram for Cu – H_2O system; [Cu] = 10^{-4} M.

I_2/I^- and IO_3^-/I^- equilibrium lines are located at higher potentials in Figure 1 with respect to the positions of Cu/Cu^{2+} and Cu/Cu_2O equilibrium lines in Figure 2. Therefore thermodynamically the IO_3^- ion can be considered as an effective oxidant for Cu.

3.2. *Expression of corrosion potential for Cu–oxidant system*

The current–potential relationship for the reaction of Cu is [24]:

$$i = 2i_o\left(\exp\left(\frac{(1+\alpha_a)F\eta_a}{RT}\right) - \exp\left(-\frac{(1-\alpha_a)F\eta_a}{RT}\right)\right) + FD_{Cu^+}\left(\frac{\partial C_{Cu^+}}{\partial x}\right)_{x=0} \quad (1)$$

Table 1. Thermodynamic data for the potential–pH diagrams in Figures 1 and 2 [24, 25]

Reactions	Log K
$HIO_4(aq) + 7H^+ + 8e^- \rightarrow I^- + 4H_2O$	164
$IO_4^- + 8H^+ + 8e^- \rightarrow I^- + 4H_2O$	166
$HIO_5^{2-} + 9H^+ + 8e^- \rightarrow I^- + 5H_2O$	174
$IO_5^{3-} + 10H^+ + 8e^- \rightarrow I^- + 5H_2O$	185
$HIO_3(aq) + 5H^+ + 6e^- \rightarrow I^- + 3H_2O$	109
$IO_3^- + 6H^+ + 6e^- \rightarrow I^- + 3H_2O$	110
$I_2(aq) + 2e^- = 2I^-$	21.0
$Cu^{2+} + 2e^- = Cu$	11.5
$2Cu^{2+} + H_2O + 2e^- = Cu_2O(s) + 2H^+$	7.0
$CuO(s) + 2H^+ = 2Cu^{2+} + H_2O$	7.3

where i_o is the exchange current density for the oxidation of Cu^+ to Cu^{2+}, α_a is the apparent charge transfer coefficient for the anodic reaction, F is the Faraday constant, R is the universal gas constant, T is the absolute temperature, η_a ($\eta_a = E_{corr} - E_{eqm,Cu^+/Cu^{2+}}$) is the anodic overpotential, D_{Cu^+} is the diffusion coefficient of Cu^+ and C_{Cu^+} is the surface Cu^+ ion concentration. At the corrosion potential, the current expression in Equation 1 will be equal to the corrosion current (i_{corr}). If the second exponential term in Equation 1 is neglected for the anodic reaction, then the corrosion potential (E_{corr}) can be expressed as:

$$E_{corr} = E_{eqm,Cu^+/Cu^{2+}} + \frac{RT}{(1+\alpha_a)F}\ln\left(\frac{i_{corr} - FD_{Cu^+}\frac{C_{Cu^+}}{\delta}}{2i_o}\right) \quad (2)$$

where $E_{eqm,Cu^+/Cu^{2+}}$ is the equilibrium potential for the oxidation of Cu^+ to Cu^{2+} and δ is the diffusion layer thickness which can be expressed by [26]:

$$\delta = 1.61 D_{Cu^+}^{1/3} \upsilon^{1/6} \omega^{-1/2} \quad (3)$$

At steady-state conditions, the corrosion current will also be equal to the cathodic current (i_c) at the corrosion potential. Substitution of δ from Equation 3 yields:

$$E_{corr} = E_{eqm,Cu^+/Cu^{2+}} + \frac{RT}{(1+\alpha_a)F}\ln\left(\frac{i_c - 0.62FD_{Cu^+}^{2/3}\upsilon^{-1/6}C_{Cu^+}\omega^{1/2}}{2i_o}\right) \quad (4)$$

Using Equation 4, diagnostic criteria can be developed to elucidate the reduction mechanism of an oxidant on Cu at the corrosion potential (E_{corr}). The dependence characteristics of E_{corr} on the rotation speed (ω) gives very useful information [17, 18]. If the oxidant is not effective, the cathodic process does not influence the corrosion potential of Cu. This case is illustrated in Figure 3 by assigning typical values to the parameters in Equation 4. The increase in the rotation speed, in Figure 3, results in a decrease in the corrosion potential. If the cathodic process is effective, however, the dependence of E_{corr} on rotation speed is directly related to the reduction mechanism of an oxidant:

Case 1. *If the cathodic reaction is diffusion-controlled:*

The cathodic current can be expressed by

$$i_c = 0.62 n_{ox} F D_{ox}^{2/3} \upsilon^{-1/6} C_{ox} \omega^{1/2} \quad (5)$$

where n_{ox} is the number of electrons in the cathodic reaction, D_{ox} and C_{ox} are the diffusion coefficient and concentration of oxidant, respectively. In this case, the corrosion potential expression becomes:

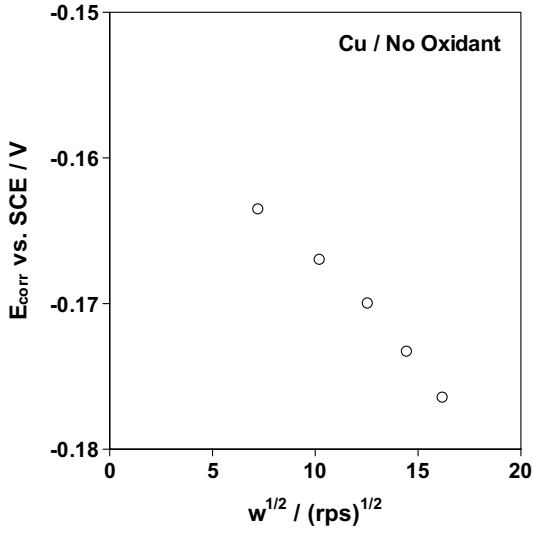

Fig. 3. The effect of rotation speed, according to Equation 4, on the corrosion potential of Cu in the absence of an oxidant. Assumptions for the parameters in Equation 4: $E_{eqm,Cu^+/Cu^{2+}} = -0.19$ V, $R = 8.314\,\mathrm{J\ (mol\,K)^{-1}}$, $T = 298\,\mathrm{K}$, $F = 96,500C$, $\alpha_a = 0.25$ [24], $i_c = 10^{-4}\,\mathrm{A\,cm^{-2}}$, $D_{Cu^+} = 10^{-5}\,\mathrm{cm^2\,s^{-1}}$, $\upsilon = 0.01\,\mathrm{cm^2\,s^{-1}}$, $C_{Cu^+} = 4\times10^{-8}\,\mathrm{mol\,cm^{-3}}$ and $i_o = 10^{-5}\,\mathrm{A\,cm^{-2}}$ [24].

$$E_{corr} = E_{eqm,Cu^+/Cu^{2+}} + \frac{RT}{(1+\alpha_a)F}\ln\left(\frac{0.62F\upsilon^{-1/6}(n_{ox}D_{ox}^{2/3}C_{ox} - D_{Cu^+}^{2/3}C_{Cu^+})\omega^{1/2}}{2i_o}\right) \quad (6)$$

The variation of E_{corr} with $\omega^{1/2}$ according to Equation 6 is depicted in Figure 4 for three different concentrations

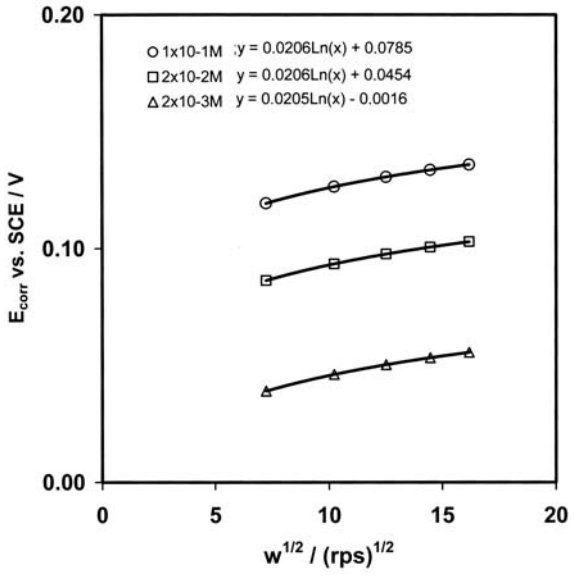

Fig. 4. The effect of rotation speed, according to Equation 6, on the corrosion potential of Cu for various oxidant concentrations, if the reduction of an oxidant is diffusion-controlled. Assumptions (in addition to the ones made for Equation 4) for the parameters in Equation 6: $n_{ox} = 1$ and $D_{ox} = 10^{-5}\,\mathrm{cm^2\,s^{-1}}$.

of the hypothetical oxidant. The increase in oxidant concentration shifts the corrosion potential in the noble direction. Equation 6 suggests that E_{corr} increases linearly with $\ln \omega^{1/2}$ with a constant slope of $RT/(1+\alpha_a)F$. In fact, the logarithmic fit of E_{corr} vs. $\omega^{1/2}$ data in Figure 4 gives constant slope for various concentrations of the oxidant.

Case 2. *If the cathodic reaction is kinetic-controlled:*

The cathodic current will be in the form:

$$i_c = n_{ox} F k C_{ox}^m \exp\left(\frac{-\alpha_{ox} z F \eta_c}{RT}\right) \tag{7}$$

where k is the apparent rate constant, m is the reaction order with respect to oxidant, α_{ox} is the apparent charge transfer coefficient for an oxidant and z is the number of electrons in the rate determining step of the cathodic reaction. Combination of Equations 4 and 7 gives the following expression:

$$E_{corr} = E_{eqm,Cu^+/Cu^{2+}} + \frac{RT}{(1+\alpha_a)F} \ln \left(\frac{n_{ox} F k C_{ox}^m \exp\left(\frac{-\alpha_{ox} z F \eta_c}{RT}\right) - 0.62 F \upsilon^{-1/6} D_{Cu^+}^{2/3} C_{Cu^+} \omega^{1/2}}{2 i_o} \right) \tag{8}$$

According to Equation 8 there cannot be an analytical expression for E_{corr} since the exponential term in the right hand side of Equation 8 also includes the parameter E_{corr} ($\eta_c = E_{corr} - E_{eqm,oxidant}$). E_{corr} values from Equation 8, however, can be obtained by the method of iteration. The variation of E_{corr}, which is obtained by iteration, with $\omega^{1/2}$ is presented in Figure 5 for two different kinds of oxidant (the rate constants (k) are different) for various oxidant concentrations. Figure 5 shows that there is no influence of rotation speed on the corrosion potential of Cu. The increase in oxidant concentration, however, increases the corrosion potential for both kinds of oxidant.

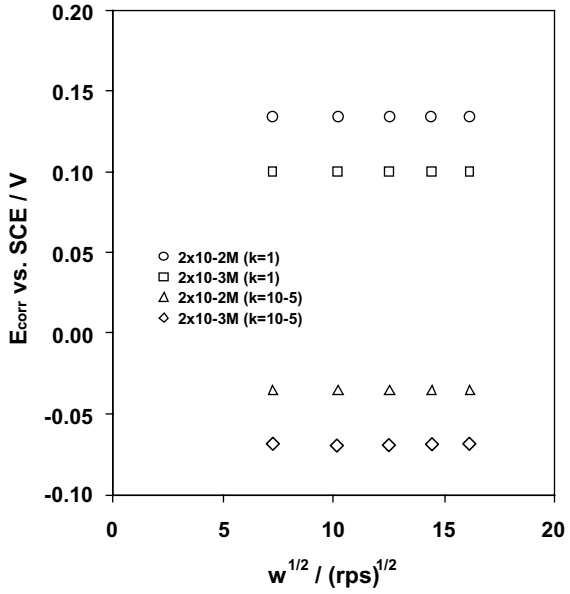

Fig. 5. The effect of rotation speed, according to Equation 8, on the corrosion potential of Cu for various oxidant concentrations, if the reduction of an oxidant is kinetic-controlled. Assumptions (in addition to the ones made for Equations 4 and 6) for the parameters in Equation 8: $E_{eqm,oxidant} = 0\,V$, $m = 1$, $\alpha_{ox} = 0.5$, $z = 1$ and, $k = 1\,cm\,s^{-1}$ for the first oxidant and $k = 10^{-5}\,cm\,s^{-1}$ for the second oxidant.

Case 3. *If the cathodic reaction is under mixed diffusion and kinetic control:*

The cathodic current, for the first order reaction, is expressed as [26]:

$$\frac{1}{i_c} = \frac{1}{i_D} + \frac{1}{i_K} \tag{9}$$

The diffusion current (i_D) is as in Equation 5 and the kinetic current (i_K) is as in Equation 7. The corrosion potential, in this case, can be expressed as in Equation 10:

$$E_{corr} = E_{eqm,Cu^+/Cu^{2+}} + \frac{RT}{(1+\alpha_a)F} \ln \left(0.62 F \upsilon^{-1/6} \left(\frac{n_{ox} k D_{ox}^{2/3} C_{ox}^m \exp\left(\frac{-\alpha_{ox} z F \eta_c}{RT}\right)}{k C_{ox}^{m-1} \exp\left(\frac{-\alpha_{ox} z F \eta_c}{RT}\right) + 0.62 \upsilon^{-1/6} D_{ox}^{2/3} \omega^{1/2}} - D_{Cu^+}^{2/3} C_{Cu^+} \right) \omega^{1/2} \right) - \frac{RT}{(1+\alpha_a)F} \ln 2 i_o \tag{10}$$

Equation 10 also suggests that there is no analytical expression for E_{corr} and the rotation speed dependence of E_{corr} is complicated. The variation of E_{corr}, obtained by the method of iteration, with $\omega^{1/2}$ is given in Figure 6 for various oxidant concentrations. The increase in rotation speed results in an increase in E_{corr}. Contrary to the case in Figure 4, however, the logarithmic fit of data does not provide a constant slope in Figure 6. In other words, the rotation speed dependence of E_{corr} varies with the oxidant concentration.

3.3. *Corrosion potential measurements in the Cu–IO_3^- system*

The variation in the stable corrosion potential values (E_{corr}) with rotation speed for various IO_3^- concentrations at pH 2, 2.5, 3 and 5 are presented in Figures 7–10, respectively. At all pH values, E_{corr} of Cu decreases as the rotation speed increases in the absence of IO_3^- (0 M) as in the case depicted in Figure 3. Figure 7 shows that the addition of IO_3^- at pH 2 causes corrosion potentials to shift in the noble direction. Also, contrary to the trends in the absence of IO_3^-, E_{corr} increases as the rotation speed increases in the presence of IO_3^- and this trend becomes more pronounced as the IO_3^- concentra-

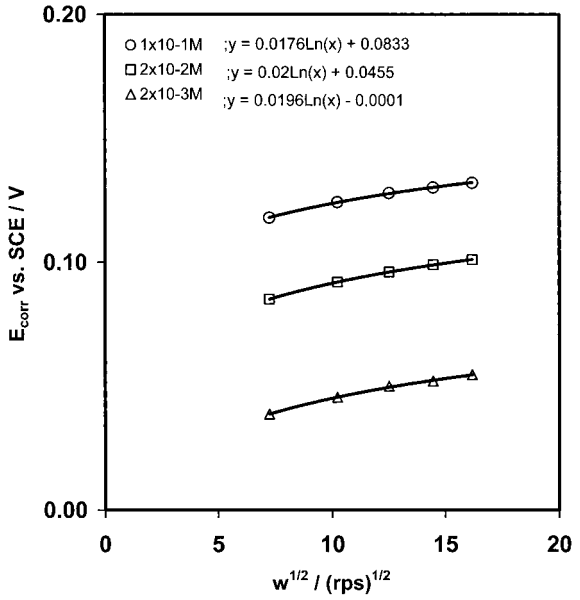

Fig. 6. The effect of rotation speed, according to Equation 10, on the corrosion potential of Cu for various oxidant concentrations, if the reduction of an oxidant is under mixed control of diffusion and kinetics. Same assumptions made for Equations 4, 6 and 8 are used for Equation 10.

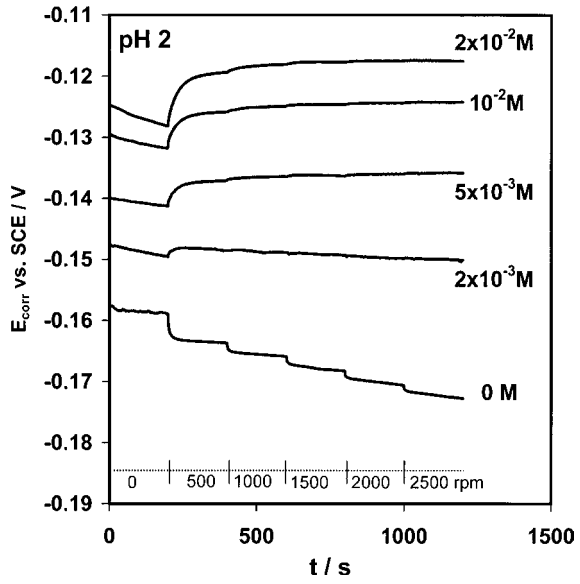

Fig. 7. The effect of rotation speed on the stable corrosion potentials of Cu for various IO_3^- concentrations at pH 2.

tion increases. At pH 2.5, in Figure 8, the addition of IO_3^- is less effective in shifting E_{corr} in the noble direction and the increase in E_{corr} with increase in rotation speed commences above 5×10^{-3} M IO_3^-. Figures 9 and 10 illustrate that addition of IO_3^- cannot change E_{corr} of Cu considerably at pH 3 and 5, respectively, and as the rotation speed increases, E_{corr} decreases as in Figure 3.

According to Figures 7–10, there are two pH regimes for the Cu–IO_3^- system: below pH 3 and above pH 3. Below pH 3 IO_3^- is an effective oxidant for Cu and the cathodic process dominates over the anodic. The reduction characteristics of IO_3^- in this regime at the corrosion

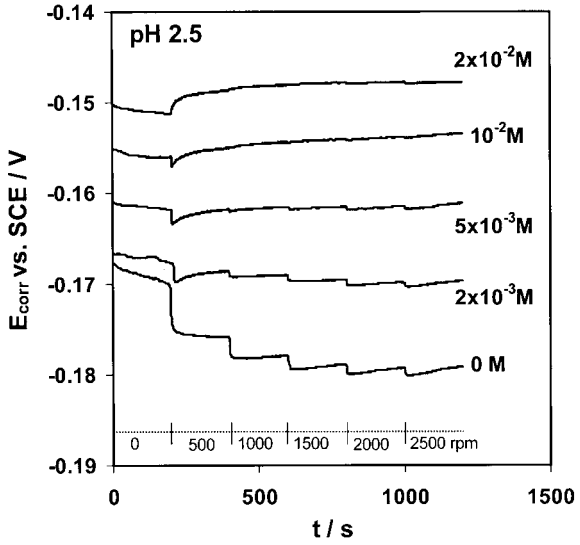

Fig. 8. The effect of rotation speed on the stable corrosion potentials of Cu for various IO_3^- concentrations at pH 2.5.

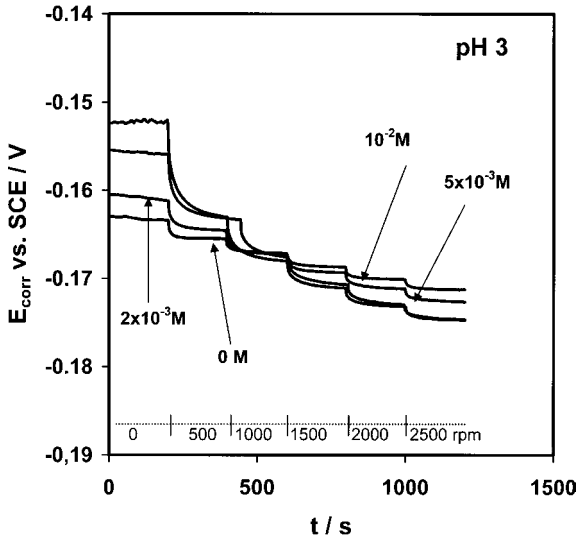

Fig. 9. The effect of rotation speed on the stable corrosion potentials of Cu for various IO_3^- concentrations at pH 3.

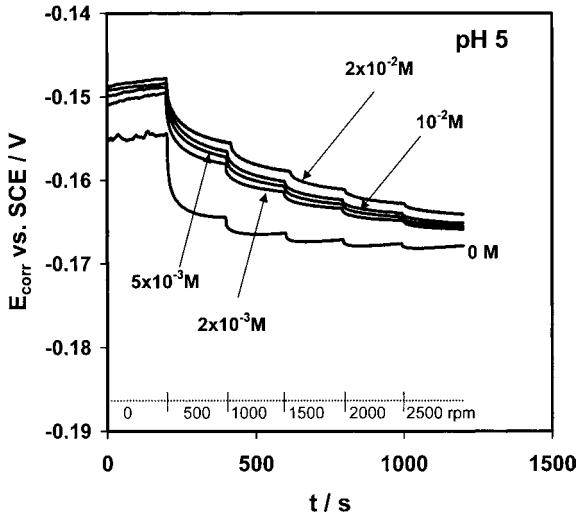

Fig. 10. The effect of rotation speed on the stable corrosion potentials of Cu for various IO_3^- concentrations at pH 5.

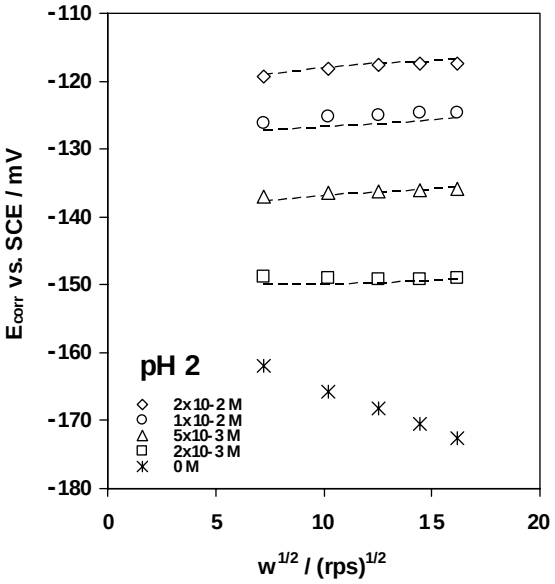

Fig. 11. E_{corr} vs. $\omega^{1/2}$ data for various IO_3^- concentrations at pH 2. Dashed lines show the fit of data according to Equation 10. Assumptions (in addition to the ones previously made for Equation 4) for the IO_3^-/I^- system: $E_{eqm,oxidant} = 1.085 - 0.059pH$, $n_{ox} = 6$, $D_{ox} = 10^{-5}\,cm^2\,s^{-1}$, $z = 1$ [25] and $m = 0.4$ (M. Anik, submitted). If $\alpha_{ox} = 0.3$, the fit of data provides $k = 3 \times 10^{-11}\,cm^{-0.8}\,s^{-1}\,mol^{0.6}$ and if $\alpha_{ox} = 0.05$, same fit of data provides $k = 4 \times 10^{-7}\,cm^{-0.8}\,s^{-1}\,mol^{0.6}$.

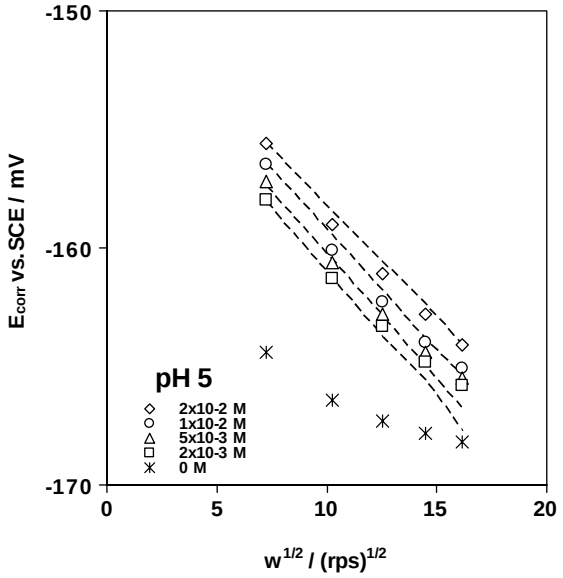

Fig. 12. E_{corr} vs $\omega^{1/2}$ data for various IO_3^- concentrations at pH 5. Dashed lines show the fit of data according to Equation 4. For pH 5: $C_{Cu^+} = 7 \times 10^{-9}\,mol\,cm^{-3}$, $i_o = 5 \times 10^{-7}\,A\,cm^{-2}$ [24] and previously used values of the other parameters in Equation 4 were re-substituted. The fit of data is possible if the values of i_C change between 5.6×10^{-7} and $6.0 \times 10^{-7}\,A\,cm^{-2}$ in Equation 4.

potential can be determined with the help of criteria developed in the previous section. Using the data in Figure 7, E_{corr} vs $\omega^{1/2}$ data are generated for pH 2 as given in Figure 11. E_{corr} increases with rotation speed in the presence of IO_3^- and as the IO_3^- concentration increases this trend becomes more significant. In other words logarithmic fit of data in Figure 11 does not give a constant slope for all IO_3^- concentrations. This observation coincides with the situation in Case 3 that the cathodic reaction is under mixed kinetic and diffusion control. In fact, previous work conducted in this laboratory [27] showed that below pH 3, IO_3^- reduction on Cu is under mixed control of the kinetics of direct reduction of IO_3^- and diffusion of I_2 (aq) from bulk solution to the electrode surface. The corrosion potential measurements also support this mechanism at the corrosion potential.

Above pH 3 IO_3^- is not an effective oxidant for Cu and the anodic process dominates over the cathodic (Figures 9 and 10). This result can be illustrated better if E_{corr} vs $\omega^{1/2}$ data are generated as in Figure 12 with the use of data in Figure 10. Previous work [27] also supports this observation that addition of IO_3^- does not influence the Cu corrosion current in this pH regime. Only after a certain cathodic overpotential does the reduction of IO_3^- become notable and the cathodic current is then controlled by slow diffusion of H^+ from bulk solution to the electrode surface [27]. Therefore IO_3^- is not a convenient oxidant for Cu CMP with weakly acidic ($pH > 3$) slurries.

Dashed lines in Figures 11 and 12 illustrate the fit of data according to Equations 10 and 4, respectively. At pH 2 (Figure 11) the fit of data provides the apparent rate constant as $4 \times 10^{-7}\,cm^{-0.8}\,s^{-1}\,mol^{0.6}$, for the IO_3^- reduction on Cu at the corrosion potential, if α_{ox} is taken as 0.05 as in the previous study [27]. This value is very close to that obtained at -800 mV previously ([27]; $10^{-6}\,cm^{-0.8}\,s^{-1}\,mol^{0.6}$). The fit of pH 5 data in Figure 12 shows that a 10 fold increase in the IO_3^- concentration causes a very slight increase in the cathodic current (from 5.6×10^{-7} to $6.0 \times 10^{-7}\,A\,cm^{-2}$). This negligible change in the cathodic current is also evidence for the strong anodic control at the corrosion potential in the Cu–IO_3^- system at pH 5.

4. Summary and conclusions

Diagnostic criteria were developed based on mixed potential theory to understand the reduction mechanism of the CMP oxidants on Cu. Copper corrosion potentials were measured in IO_3^--containing solutions for various IO_3^- concentrations and pH, and the diagnostic criteria were applied in order to determine the reduction characteristics of IO_3^- on Cu. The results obtained can be highlighted, as summarized below:

- If the anodic process dominates over the cathodic process the Cu corrosion potential decreases with rotation speed. If the cathodic process dominates, however, the rotation speed dependence of the Cu corrosion potential is directly related to the reduction mechanism of an oxidant on the Cu surface.
- If the cathodic reaction is diffusion controlled, the Cu corrosion potential increases linearly with $\ln \omega^{1/2}$.

- If the cathodic reaction is kinetically controlled, the Cu corrosion potential does not change with $\omega^{1/2}$. As the oxidant concentration increases, however, the corrosion potential shifts to more noble potentials.
- If the cathodic reaction is under mixed diffusion and kinetic control, the Cu corrosion potential increases with $\omega^{1/2}$. This increase in potential, however, is not linear with ln $\omega^{1/2}$.
- Measurements of the corrosion potential of Cu showed that addition of IO_3^- did not influence the corrosion potential significantly above pH 3 and the anodic process dominated over the cathodic process.
- Below pH 3, however, IO_3^- was found to be an effective oxidant for Cu. The reduction of IO_3^- was under mixed diffusion and kinetic control at the corrosion potential in this pH regime.

Acknowledgement

This work was supported by the Turkish State Planning Organization (Project Number: 2002K120550).

References

1. S.P. Murarka, 'Metallisation' (Butterworth-Heinemann, Boston, 1997), p. 209.
2. J.M. Steigerwald, S.P. Murarka and R.J. Gutmann, 'Chemical Mechanical Planarization of Microelectronic Materials' (Wiley, New York 1997), p. 209.
3. F.B. Kaufman, D.B. Thompson, R.E. Broadie, M.A. Jaso, W.L. Guthrie, D.J. Pearson and M.B. Small, *J. Electrochem. Soc.* **138** (1991) 3460.
4. J. Warnock, *J. Electrochem. Soc.* **138** (1991) 2398.
5. S.R. Runnels, *J. Electrochem. Soc.* **141** (1994) 1900.
6. G. Nanz and L.E. Camilletti, *IEEE Trans. Semicond. Manuf.* **8** (1995) 382.
7. N. Elbel, B. Neureither, B. Ebersberger and P. Lahnor, *J. Electrochem. Soc.* **145** (1998) 1659.
8. D. Boning, B. Lee, C. Oji, D. Ouma, T. Park, T. Smith and T. Tugbawa, *in* S.V. Babu, S. Danyluk, M. Krishnan and M. Tsujimura (Eds), 'Chemical Mechanical Polishing-Fundamentals and Challenges', Vol. 566 (MRS, Warrendale, PA, 2000), p. 197.
9. S. Basak, K. Misra, B. Withers and K. Rajeshwar, in S. Raghavan and I. Ali (Eds), 'First Int. Symp. Chemical Mechanical Planarization', Vol. 96–22 (Electrochem. Soc., Pennington, NJ, 1997), p. 137.
10. E.A. Kneer, C. Raghunath, V. Mathew, S. Raghavan and J.S. Jeon, *J. Electrochem. Soc.* **144** (1997) 3041.
11. D.J. Stein, D. Hetherington, T. Guilinger and J.L. Cecchi, *J. Electrochem. Soc.* **145** (1998) 3190.
12. D.J. Stein, D.L. Hetherington and J.L. Cecchi, *J. Electrochem. Soc.* **146** (1999) 376.
13. D. Tamboli, S. Seal, V. Desai and A. Maury, *J. Vac. Sci. Technol. A* **17** (1999) 1168.
14. H.S. Kuo and W.T. Tsai, *J. Electrochem. Soc.* **147** (2000) 2136.
15. Y. Ein-Eli, A. Abelev, E. Rabkin and D. Starosvetsky, *J. Electrochem. Soc.* **150** (2003) C646.
16. K.J. Vetter, 'Electrochemical Kinetics' (Academic Press, New York, 1967), p. 732.
17. G.P. Power and I.M. Ritchie, *Electrochim. Acta* **26** (1981) 1073.
18. G.P. Power and I.M. Ritchie, *Electrochim. Acta* **27** (1981) 165.
19. J. Li, T. Zhang and M.E. Wadsworth, *Hydrometallurgy* **29** (1992) 47.
20. H. van Kranenburg and P.H. Woerlee, *J. Electrochem. Soc.* **145** (1998) 1285.
21. Y.L. Wang, C. Liu, C. Liu, M.S. Feng and W.T. Tseng, *Mat. Chem. Phy.* **52** (1998) 17.
22. M. Anik and K. Osseo-Asare, *in* YA. Arimoto, R.L. Opila, C.R. Simpson, K.B. Sundaram, I. Ali and Y. Homma (Eds), 'Chemical Mechanical Polishing in IC Device Manufacturing III', PV 1999-37 (Electrochem. Soc. Proc. Pennington, NJ, 2000), p. 354.
23. M. Anik and K. Osseo-Asare, *in* P.C. Andricacos, J.L. Stickney, P.C. Searson, C. Reidsema-Simpson and G.M. Oleszek (Eds), 'Electrochemical Processing in ULSI Fabrication III', PV 2000-8 (Electrochem. Soc. Proc. Pennington, NJ, 2002), p. 234.
24. U. Bertocci and D.R. Turner, *in* A.J. Bard (Ed), 'Encyclopedia of Electrochemistry of the Elements', Vol. 6 (Marcel Dekker, New York, 1977), p. 383.
25. P.G. Desideri, L. Lepri and D. Heimler, *in* A.J. Bard (Ed), 'Encyclopedia of Electrochemistry of the Elements', Vol. 1 (Marcel Dekker, New York, 1973), p. 91.
26. A.J. Bard and L.R. Faulkner, 'Electrochemical Methods', (Wiley, New York, 1980), p. 280.
27. M. Anik, *J. Appl. Electrochem.* **34** (2004) 963.